Atmos. Chem. Phys., 8, 7595–7601, 2008
www.atmos-chem-phys.net/8/7595/2008/

Atmospheric Chemistry and Physics

High spatial resolution measurements of NO_2 applying Topographic Target Light scattering-Differential Optical Absorption Spectroscopy (ToTaL-DOAS)

E. Frins[1], **U. Platt**[2], **and T. Wagner**[3]

[1]Instituto de Física, Facultad de Ingeniería, J. Herrera y Reissig 565, 11300 Montevideo, Uruguay
[2]Institut für Umweltphysik, University of Heidelberg, Im Neuenheimer Feld 229, 69120 Heidelberg, Germany
[3]Max-Planck-Institut für Chemie, Becherweg 27, 55128 Mainz, Germany

Received: 15 April 2008 – Published in Atmos. Chem. Phys. Discuss.: 2 June 2008
Revised: 20 November 2008 – Accepted: 20 November 2008 – Published: 17 December 2008

Abstract. Topographic Target Light scattering – Differential Optical Absorption Spectroscopy (ToTaL-DOAS), also called Target-DOAS, is a novel experimental procedure to retrieve trace gas concentrations present in the low atmosphere. Scattered sunlight (diffuse or specular) reflected from natural or artificial targets located at different distances are analyzed to retrieve the spatial distribution of the concentration of different trace gases like NO_2, SO_2 and others. We report high spatial resolution measurements of NO_2 mixing ratios in the city of Montevideo (Uruguay) observing three buildings as targets with a Mini-DOAS instrument. Our instrument was 146 m, 196 m, and 280 m apart from three different buildings located along a main Avenue. We obtain temporal variation of NO_2 mixing ratios between 30 ppb and 65 ppb from measurements of November 2007 and mixing ratios up to 50 ppb from measurements of August and September 2008. Our measurements demonstrate that ToTaL-DOAS observations can be made over relative short distances. In polluted air masses, the retrieved absorption signal was found to be sufficiently strong to allow measurements over distances in the range of several tens of meters.

1 Introduction

Monitoring dispersion of trace gases in the troposphere near the earth surface is a challenge, in particularly when mobile emission sources are involved and the area of interest has complicated topographic structures. This is usually the case in the surroundings of a busy road in a city. High temporal and spatial resolution is desirable to describe trace gas dispersion at these sites properly. The first requirement is achieved by several passive and active optical detection methods. The second condition, i.e. the spatial resolution, is also fulfilled by some very well established optical techniques like LIDAR (e.g. Collis, 1996; Klett, 1981; Fernald, 1984) and Tomographic-DOAS (see e.g., Veitel et al., 2002; Laepple et al., 2004; Pundt et al., 2005; Hartl et al., 2006; Hashmonay et al., 1999). Unfortunately their application is associated with high expenses and staff requirements.

Topographic Target Light scattering-DOAS (ToTaL-DOAS or Target-DOAS) (Frins et al., 2006a, b; Louban et al., 2007) is a new experimental procedure to retrieve trace gas concentrations in the atmosphere near the earth surface. The method consists of pointing a passive DOAS instrument at different targets, which are illuminated by direct and/or scattered sunlight. Applying a DOAS analysis to the obtained spectra one retrieves the slant column densities (the integrated trace gas concentration) along several path segments of known length, which, in turn, allows us to derive the average trace gas concentrations. The spectral analysis varies depending on the number and sort of selected targets (bright, mixed or dark targets). A detailed description of the method is given in Frins et al. (2006a).

In early works we reported the application of this method to very large areas (Frins et al., 2006a) and to remote measurements (Louban et al., 2007), i.e. sites located far away from our instrument. The purpose of the present work is to explore the spatial resolution of ToTaL-DOAS using targets at short distances.

Correspondence to: E. Frins
(efrins@fing.edu.uy)

Published by Copernicus Publications on behalf of the European Geosciences Union.

(a)

(b)

Fig. 1. **(a)** View of the site from above, taken from www.googleearth.com. The arrows indicate the position of Targets 1, 2 and 3, respectively. At the origin of the arrows the Mini-DOAS instrument is located. **(b)** View of the targets from the instrument location.

2 ToTaL-DOAS measurements

2.1 Site description and instrument

We selected as area of interest a main street of Montevideo city (Italia Avenue), which is predominantly affected by mobile sources, since it is used by most of the private and public transport to drive in and out of the city. As measurement instrument we used a Mini MAX-DOAS instrument (Bobrowski, 2005 and Bobrowski et al., 2007), which consists of a small commercial temperature controlled fibre-optic spectrometer with a spectral resolution of 0.55 nm and a spectral range from 310–460 nm. To reduce the dark current of the detector the entire spectrometer was cooled to a stabilised temperature of +6°C. The light is coupled into the spectrometer through a quartz lens (f=40 mm, diameter=20 mm) and a quartz fibre bundle. The field of view is approximately 0.4°. The instrument is mounted on a tripod and can be pointed at different targets. It can also be oriented to elevation angles between approximately 0° and 90°. To make sure that our instrument was pointing to a specific target, a reflex sight was installed.

We located our instrument in a Park at one side of Italia Avenue, approximately 22 m away from the border of the lane (Fig. 1a). Three (almost) white walls of three different buildings at the other side of the street were selected as bright targets, i.e. the radiance reflected by these targets is assumed to be much higher than that due to scattered sunlight coming from the region between targets and instrument. These buildings were located at distances of 146 m, 196 m and 280 m from our instrument (Fig. 1b). We will call these buildings Target 1, Target 2 and Target 3, respectively.

A first set of measurements were performed on 6 November 2007 by alternating the view between the three far targets, i.e. three selected walls of the buildings, and a reference target placed near the instrument (see below). In addition, we also performed measurements of zenith scattered light as well as of instrumental dark current and offset under the same conditions. During the measurement period the ambient temperature was about 28°C, the pressure was 1013 mb, and the sky was clear.

A second set of measurements were performed on 29 August and 9 September 2008. On 29 August the ambient temperature was about 12°C, 1015 mb pressure and the sky was clear. On 9 September during the measurement it was sometimes partially cloudy, the temperature was about 20°C and the pressure was 1021 mb. The data acquisition was performed with the software package DOASIS (see http://www.iup.uni-heidelberg.de/bugtracker/projects/doasis/).

2.2 Spectral analysis

In order to retrieve the integrated trace gas concentration along the paths between our instrument and the targets, we decided to use a near target at a distance $d \approx 0$ m from the instrument to record a reference spectrum. For this purpose, during the measurements on 6 November 2007 we tested three casually available pieces of concrete by placing them directly in front of the Mini-DOAS instrument and orienting them as closely as possible in the same plane as the walls of the buildings in order to reflect light from the sky and the sun in the same direction. For the measurement of these reference spectra the instrument remained in the same orientation as for the measurements of the far targets. Like the far Targets 1, 2 and 3 (white painted walls), also the used pieces of concrete were for long time exposed to the same ambient conditions, so it was expected that their spectral reflectivity might also be similar. This assumption was tested by inspecting the spectral residuals from the various combinations of measurements (spectra from the buildings) and reference spectra (spectra from the pieces of concrete). It was found that for several combinations strongly increasing residual structures (up to more than 2%) towards shorter

wavelengths appeared (Fig. 2). Similar results were found if the various target spectra were analysed against the zenith sky spectrum. No clear relation between the magnitude of the residual structures and the properties of the targets was found from our limited set of combinations. However, it was found that using a piece of concrete covered by remnants of white paint led to results with smallest residuals. The systematic analysis of the spectral reflectivity of various materials and paints is an interesting and important subject and should be the subject of future studies.

In our study we circumvented this problem by carefully selecting the spectral region for the evaluation of NO_2. Two conditions were used as selection criteria: 1) the absorption cross section is high enough and 2) the residual is small, i.e. the spectral structure caused by the different spectral reflectances does not interfere with our measurements. Figure 2 shows a typical NO_2-evaluation from the spectra acquired on 6 November 2007 using the third building as target and a piece of concrete as reference; clearly, the residual decreases towards longer wavelengths. Taking in account these considerations, the spectral range for the evaluation of NO_2 was chosen between 430 nm and 460 nm.

The NO_2 slant column densities (SCD), i.e. the integrated concentration along the light path between Targets (Target 1, 2 and 3) and instrument (Mini MAX-DOAS), were derived from the spectral analysis using the software WINDOAS package (Fayt et al., 2001). The absorption cross sections of O_4 (Greenblatt et al., 1990) and NO_2 (Vandale et al., 1997) at 294 K, O_3 (Burrows et al., 1999) at 273 K and water vapor at 300 K (Rothman et al., 2005) were fitted to the logarithm of the ratios between the measured spectra of the targets and the reference spectrum. Additionally a synthetic Ring spectrum was included in the evaluation. As shown in Fig. 2, the NO_2 absorption can be clearly identified in the measured spectra indicating that in polluted air masses, rather short absorption paths are sufficient to achieve a good signal-to-noise ratio. From our observations we conclude that it is possible to achieve good signal-to-noise ratios for distances between the instrument and target (i.e. the absorption pathlength) of the order of tens of meters.

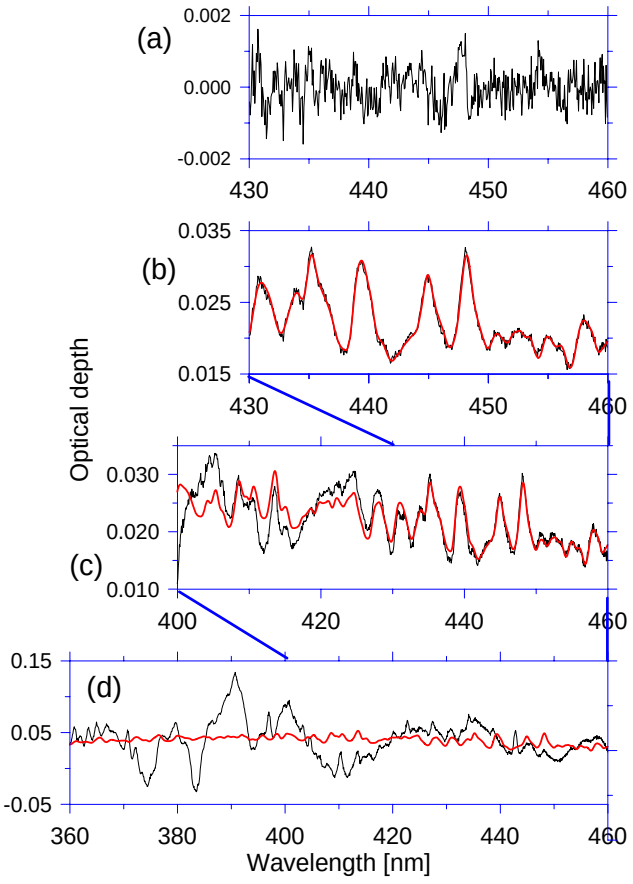

Fig. 2. Test analysis of the optimal spectral region for NO_2 evaluation of a spectrum of Target 3 (at 17:34) against a piece of concrete. **(a)** The residual for the smallest wavelength range is shown. Graphs **(b)–(d)** show the NO_2 absorption cross section (red) scaled to the NO_2 absorption detected in the measured spectrum (black).

2.3 Error estimation and detection limit

In Fig. 2 (top) also a typical residual for our NO_2 analysis is shown. It contains noise but also systematic structures. The origin of the systematic structures is not completely clear, but the most probable reason is that it is caused by remaining effects of the spectral properties of the different targets. According to Stutz and Platt (1996) we estimated the statistical error of the spectral analysis from the DOAS fit. It is typically below 5×10^{14} molec/cm^2 and thus by far smaller than the typical NO_2 slant column densities retrieved in this study. In contrast, the quantification of the systematic errors is more complicated, especially if the detailed reasons for the systematic spectral structures are not clear. We estimate the magnitude of the systematic uncertainties by conducting various sensitivity studies. First we varied the wavelength range by several nm on both sides of the selected wavelength range. In addition, we also changed the degree of the polynomial. Finally, we selected different spectra as reference spectra (besides spectra of pieces of concrete directly in front of the telescope, also a zenith sky spectrum). We found that the changes of the analysis parameters cause only changes up to $\pm4\times10^{14}$ molec/cm^2. Using the spectra of other pieces of concrete as reference spectrum yielded different results. For a piece of dark concrete, the residuals were very large (>2%) and even in the restricted wavelength range (430–460 nm) no meaningful retrieval was possible. For a second piece of bright concrete, the residual was by about a factor of 1.5 larger than that for the standard reference spectrum. The retrieved NO_2 slant column density (SCD) was only about 1×10^{14} molec/cm^2 larger than that retrieved with the standard reference spectrum. Using the zenith spectrum as reference spectrum caused residual about twice as large as with

the standard reference spectrum. The change in the retrieved NO_2 SCD was 1×10^{15} molec/cm^2. However, it should be noted that at least part of this change might also be related to temporal variations in the time between both reference spectra and to differences in the atmospheric radiation transport.

We conclude that the total error of our measurement is usually well below 5×10^{14} molec/cm^2; we use the statistical error derived from the DOAS analysis in the following. For an assumed absorption path of about 300 m (as for Target 3) we thus estimate the detection limit for the NO_2 mixing ratio to be of the order of 2 ppb.

2.4 Interpretation of the analyzed slant column densities

In first approximation, the retrieved slant column density represents the integrated trace gas concentration between the target and the instrument. This interpretation is based on the assumption that the trace gas absorptions between the top of the atmosphere and the targets (either far targets, e.g. buildings or near target, e.g. a piece of concrete) are similar and thus cancel out when rationing spectra from any of the far targets by one from the near target in the DOAS analysis. While this assumption should be quite well justified for absorptions in the upper troposphere and stratosphere, it might not be fulfilled for the trace gas absorptions close to the surface, where strong 3-dimensional gradients can occur. The potential errors introduced by such gradients are discussed and estimated in the following.

Considering the location of our instrument and the position of the targets relative to the extended emission source, there are different scenarios to be considered which could affect our interpretation: a) the emission cloud is separated from the target walls and also separated from our instrument, as depicted in Fig. 3a; b) the emission cloud encompasses the far target, so a fraction of the sunlight scattered from the targets contains additional absorption from the light path before the sun light has reached the target (Fig. 3b); c) the instrument (i.e. the near target) is reached by the emission cloud (Fig. 3c); d) the Target and our instrument are partially immersed in the emission cloud (Fig. 3d). In cases a) and d) the retrieved slant column density represents the true slant column density between the target and the instrument. In case b) the measured SCD overestimates the true SCD and in case c) it underestimates the true SCD. The associated error can be in principle be quantified by estimating the maximum difference in the vertical extension of the plume on both ends of the light path. Additional errors can be caused by horizontal gradients in the trace gas concentration above the measurement site as well as by differences in the radiative transfer conditions e.g. due to broken clouds. Typically, the resulting errors are difficult to be quantified, but a rough estimate can be gained by the measurement itself by comparing the results for targets at different distance (see Sect. 3). In general it can be assumed that the effects of spatial gradients become smaller if targets at larger distances are used.

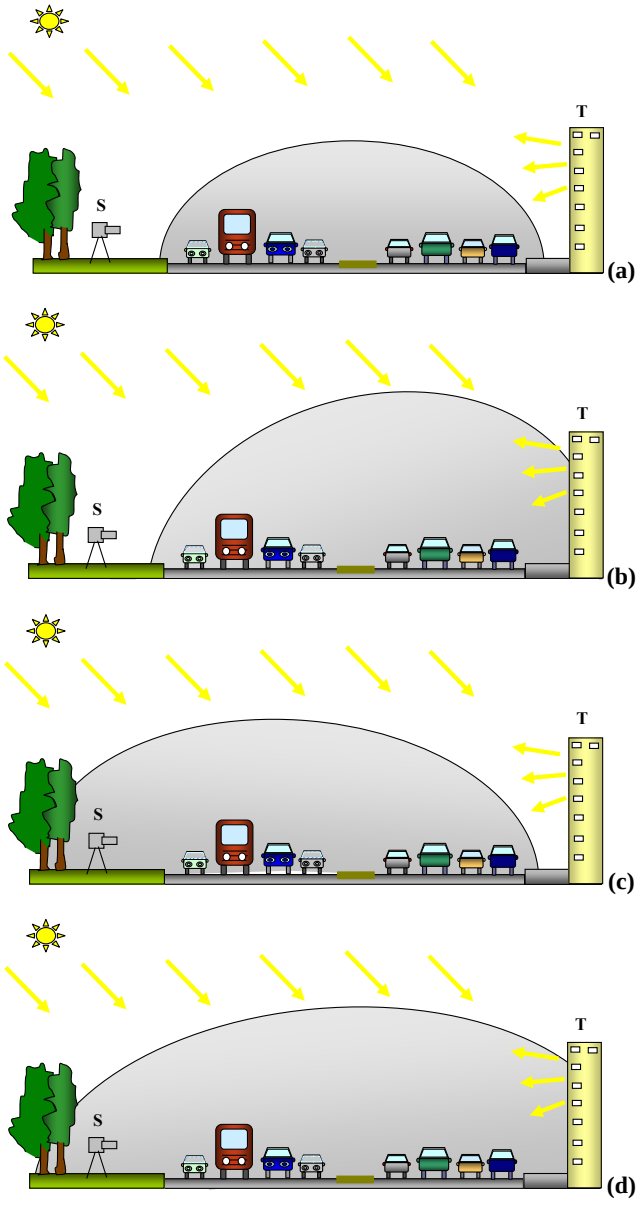

Fig. 3. Different scenarios to be considered: **(a)** Emission cloud separated from the target (T) walls and from the instrument (S); **(b)** target (T) immersed in the emission cloud; **(c)** instrument (S) immersed in the emission cloud; **(d)** target (T) and instrument (S) are immersed in the emission cloud.

In the following we simply assume that a well defined homogeneous emission cloud exists. Then, the average concentration is simply calculated by dividing the retrieved SCD by the distance between instrument and target. Dividing the obtained concentration by the concentration of air yields the averaging mixing ratio. Note that (like for long path observations) horizontal gradients might exist between the instrument and the target, which can not be resolved by the measurement.

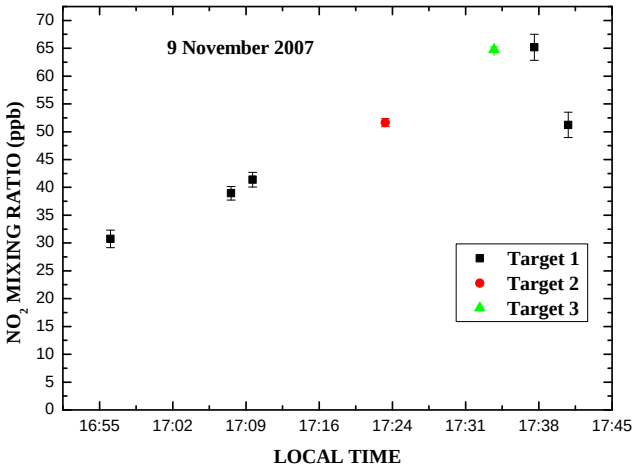

Fig. 4. Time evolution of the NO_2 mixing ratio measured on 6 November 2007.

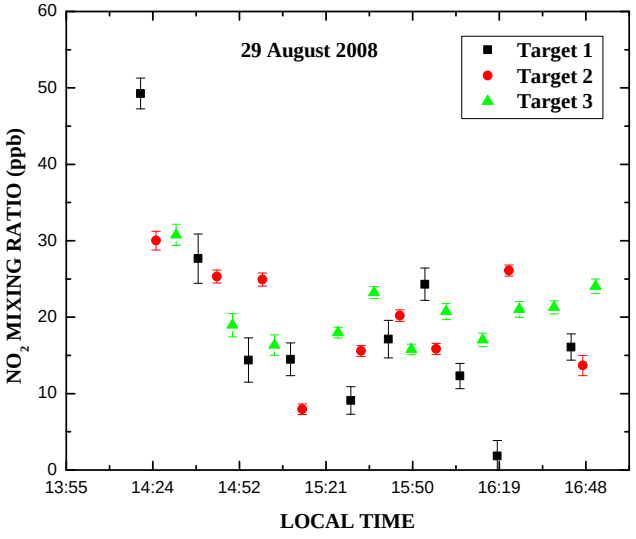

Fig. 5. Time evolution of the NO_2 mixing ratio measured on 29 August 2008.

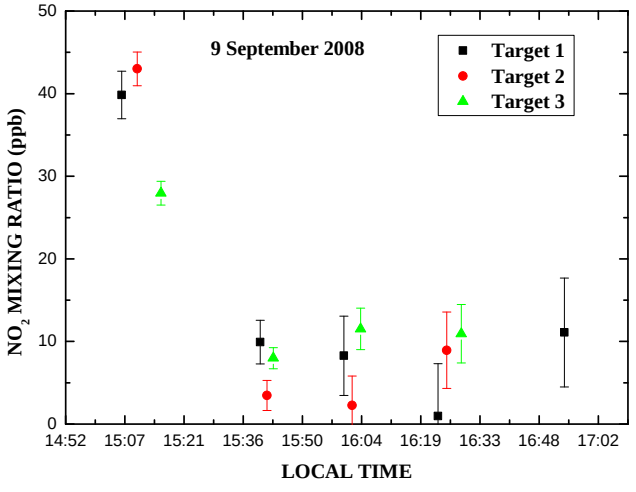

Fig. 6. Time evolution of the NO_2 mixing ratio measured on 9 September 2008.

3 Results

In the following we report average NO_2 mixing ratios derived in this way during the measurements performed on 6 November 2007, 29 August and 9 September 2008. Figure 4 shows the temporal evolution of the NO_2 mixing ratios obtained for the three different paths on 6 November 2007. As mentioned before, the measurement took place alternating between the different targets. We obtain the temporal variation of NO_2 mixing ratios between 30 ppb and 65 ppb. These temporal variations may be interpreted as a consequence of the passage of heavy vehicles like buses or trucks.

Representative slant column densities, concentration and mixing ratios of NO_2 measured between 17:24 and 17:38 local time for the different paths is summarized in Table 1.

The temporal evolution of the NO_2 mixing ratios measured on 29 August and 9 September 2008 is shown in Figs. 5 and 6, respectively. The measurements took place alternating between the same three targets used on the 6 November 2007.

In general, a similar temporal evolution of mixing ratios is retrieved for the different targets confirming the overall consistency of our assumptions. Another very important finding (mainly obvious on 29 August) is that the temporal fluctuation of the retrieved mixing ratios is by far strongest for the measurements at the closest target. In contrast, the smoothest temporal variation is found for the target at longest distance. Since these fluctuations are by far larger than the errors of the spectral retrieval (see Sect. 2.3), they can mostly be attributed to spatio-temporal variations of the NO_2 concentration field. These variations can be either caused by the gradients between the instrument and the target, or by gradients in the air masses above the instrument and the target. From our results we conclude that for a target at a distance of about 300 m (T3), the effects of these fluctuations are small (typically $<$20%). For the close target, however, sometimes even negative values are derived. Negative values indicate that not only the NO_2 concentration between instrument and target is low, but that also the SCD above the instrument (during the measurement time of the reference spectrum) was larger than that above the target (see Sect. 2.4).

4 Discussion and conclusions

We report measurements of NO_2 mixing ratios in the city of Montevideo (Uruguay) applying the ToTaL-DOAS method. We used three buildings located along a main Avenue as targets. Our Mini-DOAS instrument was only 146 m apart from

Table 1. Representative NO_2 mixing ratios measured on 6 November 2007.

Target (referred to target at d=0 m)	Local time	Slant Column Density [molec/cm^2]	Concentration [molec/cm^3]	Mixing Ratio [ppb]
Target 2 (196 m)	17:24	$2.47\times10^{16}\pm3.6\times10^{14}$	$1.26\times10^{12}\pm1.8\times10^{10}$	52±1
Target 3 (280 m)	17:34	$4.52\times10^{16}\pm3.6\times10^{14}$	$1.58\times10^{12}\pm1.3\times10^{10}$	65±1
Target 1 (146 m)	17:38	$2.32\times10^{16}\pm8.4\times10^{14}$	$1.59\times10^{12}\pm5.7\times10^{10}$	65±2

the first building, 196 m from the second and 280 m from the third one.

The first step for the evaluation of NO_2 mixing ratios was the determination of slant column densities along the segments between instrument and targets. Then, assuming that the NO_2 concentration is spatially constant in the region of interest (apart from the instrument and targets) and knowing the distance between instrument and (far) targets, it is possible to retrieve the NO_2 mixing ratios. On three days of measurements we retrieved NO_2 mixing ratios in the range between zero and 65 ppb.

Using simple assumptions on the distribution of the trace gas plume we calculated the associated errors from the uncertainty of the NO_2 slant column density retrieved from the DOAS analysis. For the shorter path (Target 1) the typical uncertainty is about 2–5 ppb, and for the longest path (Target 3) it is about 1–3 ppb. The difference for the different path lengths is physically reasonable because the actually measured quantities are the optical densities along the light paths, and thus, the signal-to-noise ratio will be smaller for the longer path lengths. Additional uncertainties are caused by fluctuations of the trace gas field. In our study, especially for the measurements at the shortest distance, differences of the NO_2 concentrations above the instrument and the target can have a strong influence on the retrieved NO_2 mixing ratio, causing occasionally even negative values. In contrast, for the target at the longest distance such effects are rather small (<20%). In general, the optimum distance should be adjusted according to the specific needs and the conditions of the particular measurement. If e.g. an isolated emission plume with zero concentrations outside has to be observed, the errors of our method should be small even for targets at very short distances.

Usually a zenith spectrum is used as reference spectrum. Instead of this, we used as reference the spectrum of a near target (in our case a piece of concrete, see above) placed directly in front of the Mini-DOAS instrument and oriented similar as the walls of the buildings in order to reflect light from the sky and the sun in the same direction. We found that some of the available pieces of concrete, exposed for long time to the same ambient conditions like the buildings (targets), have a similar spectral reflectance to those of the targets, allowing a good convergence of the spectral DOAS retrieval in the spectral range 430–460 nm. However, it should be noted that the spectral reflectances of the different targets (buildings and various pieces of concrete) showed significant differences in the wavelength ranges <430 nm. These effects should be studied in more detail in the future; probably well suited reference materials can be identified for various types of buildings and paintings to allow also a meaningful DOAS retrieval at shorter wavelengths. Alternatively, artificial, diffuse reflecting targets may be attached to buildings. From the spectral residuals of our DOAS analysis we conclude that in polluted air masses, ToTaL-DOAS measurements are possible over very short distances in the range of several tens of meters.

Furthermore, using as reference the spectrum obtained from one of the targets, it is possible to apply the ToTaL-DOAS method to evaluate trace gas concentrations in the region between several far targets. Using a well suited set of targets, it will be easily possible to apply tomographic techniques and to retrieve trace gas distributions in two or three dimensions (Hartl et al., 2006; Hashmonay et al., 1999).

Also, since the radiance received by the Mini-DOAS instrument was sufficiently high, the acquisition times were short, ranging only between 1 and 3 min depending on the target. Thus, in addition to the spatial resolution of the method, a considerable temporal resolution can be achieved.

Acknowledgements. E. Frins acknowledges PEDECIBA-Física (Project URU/06/004) for providing partial financial support.

Edited by: J. W. Bottenheim

References

Bobrowski, N.: Volcanic Gas Studies by Multi Axis Differential Optical Absorption Spectroscopy, Doctoral Thesis, University of Heidelberg, Germany, 2005.

Bobrowski, N. and Platt, U.: SO_2/BrO ratios studied in five volcanic plumes, J. Volcanol. Geotherm. Res., 3-4, 166, doi:10.1016/j.jvolgeores.2007.07.003, 147–160, 2007.

Burrows, J. P., Dehn, A., Deters, B., Himmelmann, S., Richter, A., Voigt, S., and Orphal, J.: Atmospheric Remote-Sensing Reference Data from GOME: 2, Temperature-Dependent Absorption Cross Sections of O3 in the 231–794 nm Range, J. Quant. Spectrosc. Radiat. Transf., 61, 509–517, 1999.

Collis, R. T. H.: Lidar, a new atmospheric probe, Q. J. R. Meteorol. Soc., 92, 220–230, 1966.

Fayt C. and van Roozendael, M.: WinDOAS 2.1, Software User Manual, Belgian Institute for Space Aeronomy, Brussels, Belgium (http://www.oma.be/BIRA-IASB/Molecules/BrO/WinDOAS-SUM-210b.pdf), 2001.

Fernald, F. G.: Analysis of atmospheric LIDAR observations, Some comments, Appl. Opt., 23, 652–653, 1984.

Frins, E., Bobrowski, N., Platt, U., and Wagner, T.: Tomographic multiaxis-differential optical absorption spectroscopy observations of Sun-illuminated targets, a technique providing well-defined absorption paths in the boundary layer, Appl. Opt., 45(24), 6227–6240, 2006.

Frins, E., Bobrowski, N., Platt, U., and Wagner, T.: Thomographic MAX-DOAS Observations of Sun Illuminated Targets, A New Technique Providing Well Defined Absorption Paths in the Boundary Layer or simply, Topographic Target Light scattering – DOAS ToTal – DOAS, Third International DOAS Workshop, Bremen, Germany, 2006.

Greenblatt, G. D., Orlando, J. J., Burkholder, J. B., and Ravishankara, A. R.: Absorption measurements of oxygen between 330 and 1140 nm, J. Geophys. Res., 95, 18577–18582, 1990.

Hartl, A., Song, B. C., and Pundt, I.: 2-D reconstruction of atmospheric concentration peaks from horizontal long path DOAS tomographic measurements: parametrisation and geometry within a discrete approach, Atmos. Chem. Phys., 6, 847–861, 2006, http://www.atmos-chem-phys.net/6/847/2006/.

Hashmonay, R. A., Yost, M. G., and Wu, C. F.: Computed Tomography of Air Pollutants Using Radial Scanning Path-Integrated Optical Remote Sensing, Atmos. Environ. 33(2), 267–274, 1999.

Klett, J. D.: Stable analytical inversion solution for processing LIDAR returns, Appl. Opt., 20, 211–220, 1981.

Laepple, T., Knab, V., Mettendorf, K.-U., and Pundt, I.: Longpath DOAS tomography on a motorway exhaust gas plume: numerical studies and application to data from the BAB II campaign, Atmos. Chem. Phys., 4, 1323–1342, 2004, http://www.atmos-chem-phys.net/4/1323/2004/.

Louban, I., Píriz, G., Platt, U., and Frins, E.: Differential Optical Absorption Spectroscopy (DOAS) using Targets: SO_2 and NO_2 measurements in Montevideo city, AIP Conference Proceeding, Vol. 992, 21–26, RIAO/OPTILAS, 2007.

Pundt, I., Mettendorf, K. U., Laepple, T., Knab, V., Xie, P., Lösch, J., v., Friedeburg, C., Platt, U., and Wagner, T.: Measurements of trace gas distributions using long-path DOAS-tomography during the motorway campaign BAB II: Experimental setup and results for NO2, Atmos. Environ. 39, 967–975, 2005.

Rothman, L. S., Jacquemart, D., Brown, L. R., Carleer, M., Gamache, R. R., et al.: The HITRAN 2004 Molecular Spectroscopic Database, J. Quant. Spectrosc. and Rad. Transfer, 96, 139–204, 2005.

Stutz, J. and Platt, U.: Numerical analysis and estimation of the statistical error of differential Optical absorption spectroscopy measurements with least-squares methods, Appl. Opt., 35, 6041–6053, 1997.

Vandaele, A. C., Hermans, C., Simon, P. C., Carleer, M., Colin, R., Fally, S., Mérienne, M.-F., Jenouvrier, A., and Coquart, B.: Measurements of the NO2 absorption cross section from 42000 cm-1 to 10000 cm-1 (238–1000 nm) at 220 K and 294 K, J. Quant. Spectrosc. Radiat. Transf., 59, 171–184, 1997.

Veitel, H., Kromer, B., Mößner, M., and Platt, U.: New techniques for measurements of atmospheric vertical trace gas profiles using DOAS, Environ. Sci. Pollut. Res., 4, 17–26, 2002.